Influence of Two Secondary Effects on Shear Failure of Cantilever with Attached Mass Block under Impulsive Loading*

Ya-Pu ZHAO**, Tong-Xi YU***
and Jing FANG****

The influence of two secondary effects, rotatory inertia and presence of a crack, on the dynamic plastic shear failure of a cantilever with an attached mass block at its tip subjected to impulsive loading is investigated. It is illustrated that the consideration of the rotatory inertia of the cantilever and the presence of a crack at the upper root of the beam both increase the initial kinetic energy of the block required to cause shear failure at the interface between the beam tip and the tip mass, where the initial velocity has discontinuity. Therefore, the influence of these two secondary effects on the dynamic shear failure is not negligible.

Key Words: Dynamic Failure, Transverse Shear, Cantilever, Impulsive Loading, Rotatory Inertia, Crack, Plasticity

1. Introduction

It has been found experimentally that transverse shear failure is one of the three basic failure modes of fully clamped beams[1] and fully clamped plates[2),(3)] subjected to impulsive loading. Some approximate theoretical analyses have been performed to predict the occurrence of the different failure modes. On the basis of the result of the well-known experiment by Menkes and Opat[1] on impulsively loaded ductile metal beams, Jones[4] carried out an approximate theoretical study of this problem for predicting the onset of these three failure modes. Duffy[5] found that hard-point shear failure in cylindrical shells are adequately predicted by the theory for shear failure in beams[4], by studying two loading cases (i.e., rectangular pressure pulse and exponential pressure pulse). The dynamic response and failure of fully clamped beams and circular plates were analyzed by Shen and Jones[6),(7)] using the interaction yield surface which combines bending moments, membrane force and transverse shear force. Yu considered the possibility of dynamic shear failure of a cantilever with an attached mass block at its tip subjected to impulsive loading[8]. He assuned that relative sliding occurred at the interface between the beam tip and the mass block as soon as the mass block was loaded impulsively, otherwise the shear force at the interface would be infinite. Yu also studied the influence of the rotatory inertia of the tip mass. Recently, Zhao et al.[9] theoretically investigated the dynamic plastic shear failure of an infinitely large plate with a centered cylindrical boss under impulsive loading. They showed that the influence of the rotatory inertia of the plate element on the shear failure is not negligible, and the consideration of the rotatory inertia of the plate element increases the initial kinetic energy required to cause dynamic plastic shear failure at the plate-boss interface.

Beam or cantilever is the most widely used

* Received 22nd December, 1993.
** LNM, Institute of Mechanics, Chinese Academy of Sciences, Beijing 100080, China
*** Dept. of Mechanical Eng., The Hong Kong Univ. of Sci. & Tech., Hong Kong, and Dept. of Mechanics, Peking University, Beijing 100871, China
**** Dept. of Mechanics, Peking University, Beijing 100871, China

engineering element, and the dynamic response characteristics and failure modes of beams are of important value to the response and failure analyses of other engineering elements. The background of this problem is a piece of built-in pipe struck transversely by a flying object.

It is the aim of this study to assess the influence of two secondary effects (i.e., rotatory inertia and presence of a crack) on dynamic plastic shear failure of a rigid-perfectly plastic cantilever with an attached mass block at its tip subjected to impulsive loading.

Notations

a : width of square block attached at beam tip
B : width of the cantilever
e : dimensionless kinetic energy
H : thickness of cantilever
G : mass of block
L : length of cantilever
m : mass per unit length of cantilever
M : bending moment
M_p : $YBH^2/4$, fully plastic bending moment per unit length
Q : shear force
Q_p : $YBH/\sqrt{3}$, fully plastic shear force per unit length
r : radius of gyration
t : time
V : velocity
V_0 : initial velocity of block
x : coordinate measured from the beam-block interface
y : deflection of cantilever
Y : uniaxial yield stress
α : slenderness ratio of cantilever
γ : shear strain; weakness coefficient of the cracked cross section
$\dot{\theta}$: angular velocity
Λ : length
ζ : Λ/L
ϕ : rotation
$\dot{\Omega}$: angular acceleration

2. Consideration of Rotatory Inertia of Beam

The initial configuration of the problem considered is shown in Fig. 1(a). A rigid mass block is attached to the tip of the cantilever, which is struck transversely by an impulsive load and obtains an initial velocity V_0. Parkes[10] considered the rigid perfectly plastic response of this problem. Yu has considered the dynamic plastic shear failure at the interface between the beam tip and the mass block[8]. In this section, the rotatory inertia of the beam element will be taken into account. For simplicity, the following assumptions are adopted

① The deflection of the cantilever during the deformation process is much smaller than the length of the cantilever L.

② For the cantilever with a uniform rectangular section, let H and B represent the thickness and the width of the beam, respectively. m denote the mass of the beam per unit length.

③ The material of the beam is rate-independent and rigid perfectly plastic; the rotatory inertia of the beam element is considered.

④ The rigid tip mass is a square block whose volume density and width are the same as those of the cantilever, as shown in Fig. 1(b). The rotatory inertia of the tip mass is also considered.

The square yield function shown in Fig. 2 is adopted in this paper. If the interface between the rigid and plastic zones is stationary and the stress points are located on side AB or CD, then the discontinuity conditions at this interface are given by

$$[\dot{y}]=[Q]=[M]=0. \quad (1)$$

Otherwise, the discontinuity conditions are expressed by

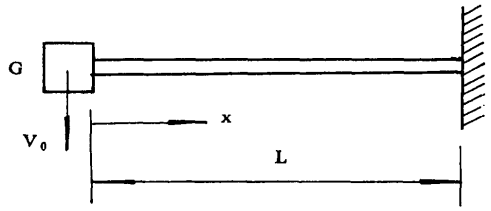

(a) Initial configuration of the structure

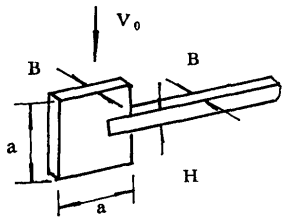

(b) Schematic illustration of the mass block

Fig. 1

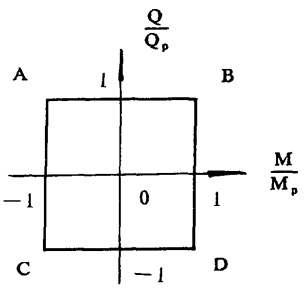

Fig. 2 Square yield function

$$[\ddot{\psi}]=[Q]=[M]=0. \quad (2)$$

Because of the discontinuity of the initial velocity at the interface between the tip mass and the cantilever, shear force is singular at this section at $t=0$, so that relative sliding occurs at the initial instant. The deformation mechanism is illustrated in Fig. 3. The equations of motion of the cantilever are

$$Q'=m\ddot{y} \quad (3.a)$$

$$M'=Q-mr^2\ddot{\psi} \quad (3.b)$$

where Q and M are the shear force and the bending moment, respectively, y is the deflection of the cantilever, $r=H/2\sqrt{3}$ is the radius of gyration, $y'=\psi+\gamma$, ψ is the rotation of lines which were originally perpendicular to the initial midplane, due to bending, and γ is the transverse shear strain.

If its rotatory inertia is taken into account, the equations of motion of the mass block may be given by[8]

$$G\dot{V}_c=-Q_p \quad (4.a)$$

$$Ga^2\dot{\Omega}/6=M_p+Q_pa/2, \quad (4.b)$$

where M_p and Q_p denote the fully plastic limit bending moment and fully plastic shear force per unit length, respectively. G is the mass of the block.

The angular acceleration and the velocity at the side adjacent to the beam tip of the mass block can be expressed by

$$\dot{\Omega}=\frac{3YBH^2}{Ga^2}\left(\frac{1}{2}+\frac{1}{\sqrt{3}}\frac{a}{H}\right) \quad (5)$$

$$V^-=V_0-\frac{YBH}{4G}\left(\frac{10}{\sqrt{3}}+3\frac{H}{a}\right)t. \quad (6)$$

Equation (6) shows that the velocity of the block at the side adjacent to the beam tip decreases linearly with time.

Since the beam is divided into two different regions, a rigid region and a plastic region, it would be convenient to study them separately.

2.1 Analysis of rigid region of beam ($0\leq x\leq\Lambda$)

It is clear that the acceleration distribution in this region is linear with x; therefore, it can be expressed as

$$\dot{V}=\dot{V}^+ +\ddot{\psi}_0x, \quad (7)$$

where $\dot{V}^+$ is the acceleration of the beam tip adjacent to the block, and $\ddot{\psi}_0$ is the angular acceleration of this rigid region.

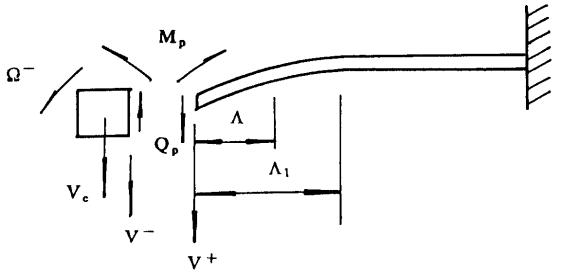

Fig. 3 Deformation mechanism

Noting that $Q=-Q_p$ at $x=0$ and using both Eqs. (3.a) and (7), one can obtain the shear force distribution as

$$Q=-Q_p+m\dot{V}^+x+m\ddot{\psi}_0x^2/2. \quad (8)$$

Substituting Eq. (8) into Eq. (3.b) and integrating, one can obtain the distribution of the bending moment given by

$$M=M_p-(Q_p+mr^2\ddot{\psi}_0)x+m\dot{V}^+x^2/2+m\ddot{\psi}x^3/6, \quad (9)$$

where the boundary condition $M=M_p$ at $x=0$ has been used.

2.2 Analysis of plastic region of beam

In this region, since the stress points are located on side AB or CD in the square yield surface, then

$$\gamma=0, \quad M'=0.$$

From Eqs. (3.a) and (3.b), we know that the acceleration of the beam in this region $\ddot{y}$ satisfies

$$\ddot{y}''-\frac{1}{r^2}\ddot{y}=0. \quad (10)$$

The general solution of the above equation can be written as

$$\ddot{y}=C_1(t)\exp(x/r)+C_2(t)\exp(-x/r). \quad (11)$$

Since $\ddot{y}\to 0$ for sufficiently large x, it is required that

$$C_1(t)\equiv 0.$$

Thus, the distribution of acceleration in this region is given by

$$\ddot{y}=C_2(t)\exp(-x/r) \quad (12)$$

It can be shown from Eqs. (3.a), (3.b) and (12) that the shear force distribution in this region is given by

$$Q=-mrC_2(t)\exp(-x/r). \quad (13)$$

2.3 Shear failure analysis

On the basis of the continuity requirements of the cantilever for acceleration, bending moment, shear force and slope, one can obtain the following equations:

$$\dot{V}^+ +\ddot{\psi}_0\Lambda=C_2(t)\exp(-\Lambda/r) \quad (14.a)$$

$$-Q_p+m\dot{V}^+\Lambda+m\ddot{\psi}_0\Lambda^2/2=-mrC_2(t)\exp(-\Lambda/r) \quad (14.b)$$

$$M_p-(Q_p+mr^2\ddot{\psi})\Lambda+m\dot{V}^+\Lambda^2/2+m\ddot{\psi}_0\Lambda^3/6=0 \quad (14.c)$$

$$\ddot{\psi}_0=-\frac{C_3(t)}{r}\exp(-\Lambda/r), \quad (14.d)$$

where $\dot{V}^+$, $\ddot{\psi}_0$, Λ and $C_2(t)$ are unknown variables.

It may be shown from Eqs. (14.a) and (14.b) that Λ satisfies the following dimensionless equation:

$$(2+\zeta^2+\zeta^3)(3\zeta+4\zeta^2-6)=2(1+\zeta)(12+\zeta^2+3\zeta^3), \quad (15)$$

where $\zeta=\Lambda/r$.

Equation (15) is solved numerically, and the value of ζ is found to be

$$\zeta=2.392, \quad (16)$$

i.e.,

$$\Lambda=0.69H. \tag{17}$$

Thus, the acceleration of the beam tip adjacent to the block is

$$\dot{V}^+=2\frac{YB}{m}\frac{1+\zeta}{1+\zeta^2/2+\zeta^3/2}$$
$$=0.634\frac{YB}{m}. \tag{18}$$

Integrating Eq. (18) and with $V^+=0$ at $t=0$, we obtain

$$V^+=0.634\frac{YB}{m}t. \tag{19}$$

Equation (19) means that the velocity of the beam tip increases linearly with time.

It is clear that the relative sliding velocity at the interface between the beam tip and the block is given by

$$[V]=V^- - V^+$$
$$=V_0-\frac{YBH}{4G}\left[\frac{10}{\sqrt{3}}+3\frac{H}{a}+2.53\left(\frac{a}{H}\right)^2\right]t. \tag{20}$$

It should be pointed out that assumption ④ has been used in Eq. (20), i.e., $m=GH/a^2$. Equation (20) shows that the relative sliding velocity at the interface decreases linearly from its initial value V_0 with time. Therefore, the total sliding displacement at the interface may be given by

$$[S]=\frac{4K_0}{YBH}\left[\frac{10}{\sqrt{3}}+3\frac{H}{a}+2.53\left(\frac{a}{H}\right)^2\right]^{-1}, \tag{21}$$

where $K_0=GV_0^2/2$ is the initial kinetic energy of the block.

Equation (21) can be written in a dimensionless form, namely,

$$[S]/H=\frac{K_0}{M_p}\left[\frac{10}{\sqrt{3}}+3\frac{H}{a}+2.53\left(\frac{a}{H}\right)^2\right]^{-1}. \tag{22}$$

Failure is considered to occur when

$$[S]/H\geq k, \tag{23}$$

where k is the material constant to be determined experimentally. It is obvious that complete severance occurs at the interface when $k=1$; however, transverse shear failure is likely to develop for a smaller value of k for beams[11]. The value of k may be larger for ductile materials and smaller for brittle materials. For convenience, $k=1$ is used in the present study; for other values of k shear failure analysis can be treated in the same manner. It is obvious, therefore, that complete shear failure occurs at the interface when

$$K_0\geq\left[\frac{10}{\sqrt{3}}+3\frac{H}{a}+2.53\left(\frac{a}{H}\right)^2\right]M_p. \tag{24}$$

For convenience, a dimensionless kinetic energy is introduced as

$$e_0=K_0/M_p. \tag{25}$$

The critical value of the dimensionless kinetic energy, e_{cr}, can then be written as

$$e_{cr}=\frac{10}{\sqrt{3}}+3\frac{H}{a}+2.53\left(\frac{a}{H}\right)^2. \tag{26}$$

When $e_0\geq e_{cr}$, dynamic plastic shear failure is considered to have occurred.

Bearing in mind that the critical dimensionless kinetic energy, when the rotatory inertia of the cantilever is neglected, has been obtained by Yu[8] as

$$e'_{cr}=\frac{10}{\sqrt{3}}+3\frac{H}{a}+1.33\left(\frac{a}{H}\right)^2, \tag{26}'$$

It is clear that the consideration of the rotatory inertia of the cantilever increases the initial kinetic energy required to cause complete shear failure at the interface between the beam tip and the mass block.

It can also be found from Eq. (14) that the angular acceleration of the rigid part of the beam is

$$\ddot{\psi}_0=-0.65\frac{YB}{G}\left(\frac{a}{H}\right)^2. \tag{27}$$

The above discussion holds if $\Omega<|\ddot{\psi}_0|$, for which it is required that

$$0.65\left(\frac{a}{H}\right)^4-\sqrt{3}\left(\frac{a}{H}\right)-1.5>0. \tag{28}$$

It is required by inequality (28) that

$$a/H>1.60. \tag{29}$$

3. Influence of Presence of a Crack

Suppose that there is a crack (or notch) at the upper root of the cantilever whose initial configuration is shown in Fig. 4. The crack weakens the cracked section to such an extent that a stationary plastic hinge develops there when the bending moment reaches a value $\gamma M_p<M_p$, where $0<\gamma\leq 1$ is a function of the crack size, with the limiting case $\gamma=1$ corresponding to no crack. The nonlinear relationship between γ and physical size depends on the cross section of the beam and the assumed geometry of the crack and may easily be determined by considering the statics of a fully yielded uncracked ligament[12),(13)]. The so-called "double-hinge model" and the square yield function, shown in Fig. 2, are used in the analysis.

The deformation mechanism is illustrated in Fig. 5. Points B and C are two stationary plastic hinges. The application of conservation of momentum and conservation of angular momentum on the system gives

$$\frac{m}{2}[\dot{V}^+ +(1-\zeta)L\ddot{\theta}_0]\zeta L=Q_p \tag{30.a}$$

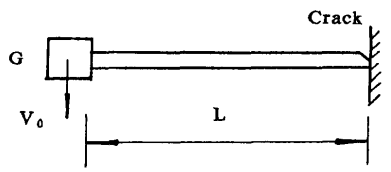

Fig. 4 Initial configuration of a cracked cantilever

$$\frac{m}{6}\zeta^2L^2[\dot{V}^+ + 2(1-\zeta)L\ddot{\theta}_0] = 2M_p \tag{30.b}$$

$$\frac{m}{3}(1-\zeta)^3L^3\ddot{\theta}_0 = (1-\gamma)M_p. \tag{30.c}$$

The position of the stationary plastic hinge C is, therefore, determined by the following dimensionless equation:

$$\zeta = \left[2 - \frac{1-\gamma}{2}\frac{\zeta^2}{(1-\zeta)^2}\right]\frac{3\sqrt{3}}{4}\alpha. \tag{31}$$

where $\alpha = H/L$ represents the slenderness ratio of the cantilever.

Equation (31) shows that the position of plastic hinge C depends on α and γ. From Eqs. (30.a)～(30. c), we also obtain

$$\ddot{\theta}_0 = \frac{3}{m}(1-\gamma)\frac{M_p}{(1-\zeta)^3L^3} \tag{32.a}$$

$$\dot{V}^+ = \frac{YB}{m}\alpha\left[\frac{2}{\sqrt{3}\zeta} - \frac{3}{4}(1-\gamma)\frac{\alpha}{(1-\zeta)^2}\right]. \tag{32.b}$$

Integrating Eq. (32.b) yields

$$V^+ = \frac{YB}{m}\alpha\left[\frac{2}{\sqrt{3}\zeta} - \frac{3}{4}(1-\gamma)\frac{\alpha}{(1-\zeta)^2}\right]t. \tag{33}$$

Equation (33) shows that the tip velocity of the cantilever increases linearly with time. Equations (5) and (6) still hold in this case. Therefore, it is easy to obtain the relative sliding velocity at the interface.

$$[V] = V_0 - \frac{YBH}{4G}\left[\frac{10}{\sqrt{3}} + 3\frac{H}{a} + \frac{8}{\sqrt{3}}\frac{\alpha}{\zeta}\left(\frac{a}{H}\right)^2 - 3\frac{(1-\gamma)}{(1-\zeta)^2}\alpha^2\left(\frac{a}{H}\right)^2\right]t \tag{34}$$

Similarly, the total dimensionless sliding displacement at the interface is expressed by

$$[S]/H = \frac{K_0}{M_p}\left[\frac{10}{\sqrt{3}} + 3\frac{H}{a} + \frac{8}{\sqrt{3}}\frac{\alpha}{\zeta}\left(\frac{a}{H}\right)^2 - 3\frac{(1-\gamma)}{(1-\zeta)^2}\alpha^2\left(\frac{a}{H}\right)^2\right]^{-1}, \tag{35}$$

where again, K_0 is the initial kinetic energy of the block.

The critical dimensionless initial kinetic energy required to cause shear failure at the interface is

$$e_{cr} = \frac{10}{\sqrt{3}} + 3\frac{H}{a} + \left[\frac{8}{\sqrt{3}}\frac{\alpha}{\zeta} - 3\frac{(1-\gamma)}{(1-\zeta)^2}\alpha^2\right]\left(\frac{a}{H}\right)^2. \tag{36}$$

If $e_0 \geq e_{cr}$, then dynamic plastic shear failure is considered to have occurred.

Since the two sides of the interface have different angular velocities, the following inequality must be satisfied.

$$\left[2 - \frac{3\sqrt{3}}{2}(1-\gamma)\frac{\alpha\zeta}{(1-\zeta)^2}\right]\left(\frac{\alpha}{\zeta}\right)^2\left(\frac{a}{H}\right)^4 - 3\frac{a}{h} - \frac{3\sqrt{3}}{2} > 0 \tag{37}$$

3.1 Numerical example

The basic data of the cantilever adopted in this example are from the famous experiment done by Parkes[10], i.e.,

Table 1 Numerical results for different γ

γ	α	ξ	ξ/α	$\frac{8}{\sqrt{3}}\frac{\alpha}{\xi} - \frac{3(1-\gamma)}{(1-\xi)^2}\alpha^2$
1.0			2.598	1.33
0.8	1/8	0.321117	2.570	1.78
	1/16	0.162071	2.593	1.78
	1/32	0.0811558	2.597	1.78
	1/48	0.054116	2.598	1.78
0.6	1/8	0.317708	2.542	1.78
	1/16	0.16177	2.588	1.78
	1/32	0.0811242	2.596	1.78
	1/48	0.0541073	2.597	1.78
0.5	1/8	0.31608	2.529	1.78
	1/16	0.161621	2.586	1.78
	1/32	0.0811084	2.596	1.78
	1/48	0.0541029	2.597	1.78

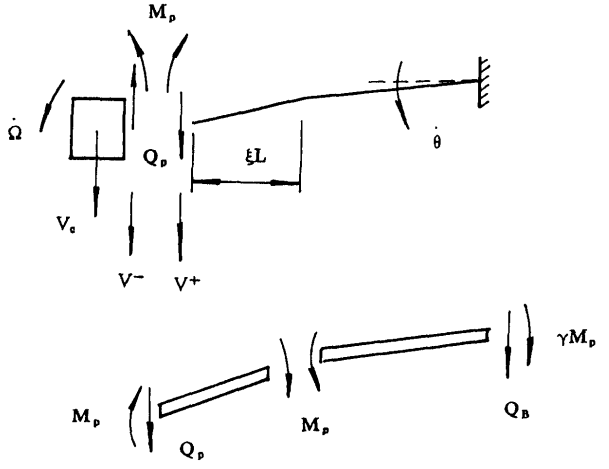

Fig. 5 Deformation mechanism of the cracked structure

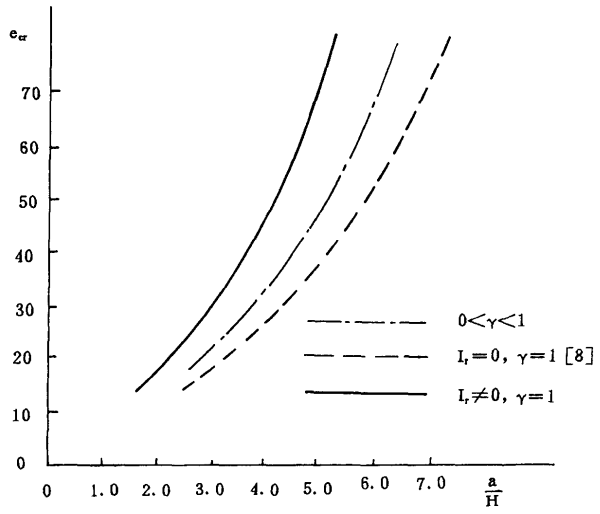

Fig. 6 Comparison of three cases

$B \times H = \frac{1''}{4} \times \frac{1''}{4}$; $L = 2'', 4'', 8''$ and $12''$.

Therefore, the slenderness ratios of the cantilevers are, respectively,

$\alpha = 1/8, 1/16, 1/32$ and $1/48$.

The results of numerical calculations for different γ, are listed in Table 1.

From Eq. (36) and Table 1, we know that the critical value of the dimensionless kinetic energy for shear failure at the interface can be simply expressed by

$$e_{cr} = \frac{10}{\sqrt{3}} + 3\frac{H}{a} + 1.78\left(\frac{a}{H}\right)^2. \tag{38}$$

Equation (38) shows that e_{cr} is insensitive to γ, the coefficient of weakness of the cracked section. From Table 1 and inequality (35), we also know that the ratio a/H must satisfy

$$a/H > 2.60. \tag{39}$$

4. Discussion and Conclusions

This paper concerns the influence of two secondary effects, rotatory inertia and presence of a crack, on the dynamic plastic shear failure of a cantilever with an attached mass block at its tip subjected to impulsive loading. Two dimensionless initial kinetic energy crieria are presented to predict the shear failure at the interface.

It has been shown that the consideration of the rotatory inertia of the beam element increases the initial kinetic energy causing shear failure at the interface between the beam tip and the tip mass, where the initial velocity has discontinuity. The comparison between considering rotatory inertia and neglecting of is illustrated in Fig. 5.

It has been also proven that the presence of a crack (or notch) at the upper root of the cantilever increases the initial kinetic energy required to cause shear failure at the interface; however, it is smaller than that when the rotatory inertia of the beam element is taken into account. The comparison of these three cases is shown in Fig. 6.

It is worthy to note that the dynamic plastic failure of a notched non-straight element (notched circular ring[14)-(16)]) may be quite different from the failure mode of a notched straight cantilever. Zhao et al. found that "Notch Sensitive Regions (NSR)" exist on the exterior surface of a circular ring rest on a arc-shaped support loaded dynamically. If a notch is out of the NSR, the notch will have not influence on the deformation and failure of the ring; if not, the notch will have strong influence on the dynamic failure of the ring.

Aknowledgment

This study was supported by the National Natural Science Foundation of China.

References

(1) Menkes, S. B. and Opat, H. J., Exp. Mech., Vol. 13 (1973), p. 480.
(2) Teeling-Smith, R. G. and Nurick, G. N., Int. J. Impact Engng, Vol. 11, No. 1 (1991), p. 77.
(3) Olson, M. D. et al., Int. J. Impact Engng, Vol. 13, No. 2 (1993), p. 279.
(4) Jones, N., Tran. ASME, J. Eng. Indus., Vol. 98 (1976), p. 131.
(5) Duffy, T. A., Structural Failure, (Wierzbicki, T. and Jones, N. eds.), Chap. 6, (1988), John Wiley & Sons, Inc.
(6) Shen, W. Q. and Jones, N., Int. J. Impact Engng, Vol. 12, No. 1 (1992), p. 101.
(7) Shen, W. Q. and Jones, N., Int. J. Impact Engng, Vol. 13, No. 2 (1993), p. 259.
(8) Yu, T. X., Explosion & Shock Waves, (in Chinese), Vol. 13, No. 2 (1993), p. 97.
(9) Zhao, Ya-Pu, Fang, J. and Yu, T. X., Int. J. Solids Structures, Vol. 31, No. 11 (1994), p. 1585.
(10) Parkes, E. W., Proc. Roy. Soc., Ser. A, Vol. 228 (1955), p. 462.
(11) Jouri, W. S. and Jones, N., Int. J. Mech. Sci., Vol. 30, No. 3/4 (1988), p. 153.
(12) Petroski, H. J., Int. J. Pres. Ves. & Piping, Vol. 13, No. 1 (1983), p. 1.
(13) Petroski, H. J., J. Appl. Mech., Vol. 51 (1984), p. 329.
(14) Zhao, Ya-Pu, Ph. D. Thesis, Peking University, (in Chinese), Chap. 6 (1994).
(15) Zhao, Ya-Pu, et al., DYMAT Journal, (in press).
(16) Zhao, Ya-Pu, et al., Int. J. Pres. Ves. & Piping, (in press).